BOREAS An international journal of Quaternary research

Southern Hemisphere Westerly Winds have modulated the formation of laminations in sediments in Lago Fagnano (Tierra del Fuego, Argentina) over the past 6.3 ka

ALEXIS VIZCAINO, FRANCISCO J. JIMENEZ-ESPEJO, ROBERT B. DUNBAR, DAVID MUCCIARONE, ANTONIO GARCÍA-ALIX, INA NEUGEBAUER AND DANIEL ARIZTEGUI

BOREAS

Vizcaino, A., Jimenez-Espejo, F. J., Dunbar, R. B., Mucciarone, D., García-Alix, A., Neugebauer, I. & Ariztegui, D.: Southern Hemisphere Westerly Winds have modulated the formation of laminations in sediments in Lago Fagnano (Tierra del Fuego, Argentina) over the past 6.3 ka. *Boreas*. https://doi.org/10.1111/bor.12600. ISSN 0300-9483.

Tierra del Fuego in Argentina is a unique location to examine past Holocene wind variability since it intersects the core of the Southern Hemisphere Westerly Winds (SHWW). The SHWW are the most powerful prevailing winds on Earth. Their variation plays a role in regulating atmospheric CO_2 levels and rainfall amounts and distribution, both today and in the past. We obtained a piston core (LF06-PC8) from Bahía Grande, a protected sub-basin at the southern margin of Lago Fagnano, the largest lake in Tierra del Fuego. This article focuses on the uppermost 185 cm of this core, corresponding to laminated sediment from the last ~6.3 ka. Laminations consist of millimetre-scale paired dark and light layers. Previous studies and new geochemical analysis show that the dark and light layers are characterized by differing concentrations of Mn and Fe. We attribute the distribution of Mn and Fe to episodic hypolimnic oxic–anoxic variations. The age model suggests an approximately bidecadal timescale for the formation of each layer pair. We propose a new model of these redox changes with the SHWW variations. The most likely phenomenon to produce complete water-column mixing is thermobaric instability, which occurs in colder winters with low-intensity SHWW (El Niño-like conditions). In contrast, windier winters are characterized by higher temperatures and reduced mixing in the water column, facilitating a decline in oxygen concentration. Laminations, and the inferred presence of periodic hypolimnion redox changes, are common features of the past ~6.3 ka. Geochemical proxy variability is compatible with an intensification of El Niño/Southern Oscillation activity during the past ~2 ka.

Alexis Vizcaino, Robert B. Dunbar and David Mucciarone, Earth System Science, Stanford University, 397 Panama Mall, Stanford, CA 94305, California, USA; Francisco J. Jimenez-Espejo (corresponding author: fjjspejo@ugr.es), Instituto Andaluz de Ciencias de la Tierra, UGR-CSIC, Avda. de las Palmeras n° 4, 18100, Armilla, Spain and Research Institute for Marine Resources Utilization (Biogeochemistry Program), Japan Agency for Marine-Earth Science and Technology, 2-15 Natsushimacho, Yokosuka, Kanagawa 237-0061, Japan; Antonio García-Alix, Department Paleontología y Estratigrafía, Universidad de Granada, Avenida de la Fuente Nueva S/N, 18071, Granada, Spain; Ina Neugebauer and Daniel Ariztegui, Department of Earth Sciences, University of Geneva, Rue des Maraichers 13, 1205, Geneva, Switzerland; Ina Neugebauer, Section Climate Dynamics and Landscape Evolution, GFZ German Research Centre for Geosciences, Wissenschaftpark "Albert Einstein", Telegrafenberg, 14473, Potsdam, Germany; *received 19th June 2021, accepted 16th July 2022.*

Lago Fagnano (LF) is the most southerly large lake outside of Antarctica, and it is a key location at which to understand the relationship between Antarctic and South American climate variations. Previous studies based on sediment cores in Lago Fagnano have allowed the reconstruction of Late Pleistocene and Holocene climate, environment, glacial fluctuations and tectonic activity (Waldmann *et al.* 2008, 2010, 2011, 2014; Moy *et al.* 2011; Sanci *et al.* 2021). Lago Fagnano's location and orientation make this site an excellent place to examine the Holocene variations of the Southern Hemisphere Westerly Winds (SHWW), because of the weaker rainshadow effect owing to the lower elevation of the Andes running parallel to the westerlies (Fig. 1). The SHWW exert strong control over the amount and distribution of rainfall (Garreaud *et al.* 2013; McCulloch *et al.* 2020) and regional vegetation (Markgraf & Huber 2010), associated with Andean orographic effects (Garreaud 2007; Moy *et al.* 2008; Lamy *et al.* 2010). The SHWW, together with human activity (agriculture and cattle farming), have a significant influence on Patagonian life and water management. Globally, the SHWW are thought to play an important role in the regulation of atmospheric CO_2 levels through: (i) a direct effect related to higher gas transfer velocities governing the air–sea gas exchange at higher wind speeds (e.g. Ito *et al.* 2010); and (ii) dynamic changes in ocean productivity and upwelling/downwelling that influence the CO_2 difference between ocean and atmosphere (Canadell *et al.* 2007; Lamy *et al.* 2010).

Many studies have focused on understanding the SHWW regime and its past latitudinal movement (e.g. Saunders *et al.* 2018; Xia *et al.* 2018). There is evidence for a northward shift or expansion of the SHWW during the Holocene (McCulloch *et al.* 2000; Toggweiler *et al.* 2006), yet we still have few details on how the winds changed and whether their strength varied by latitude. Previous insights are derived from glacial

DOI 10.1111/bor.12600

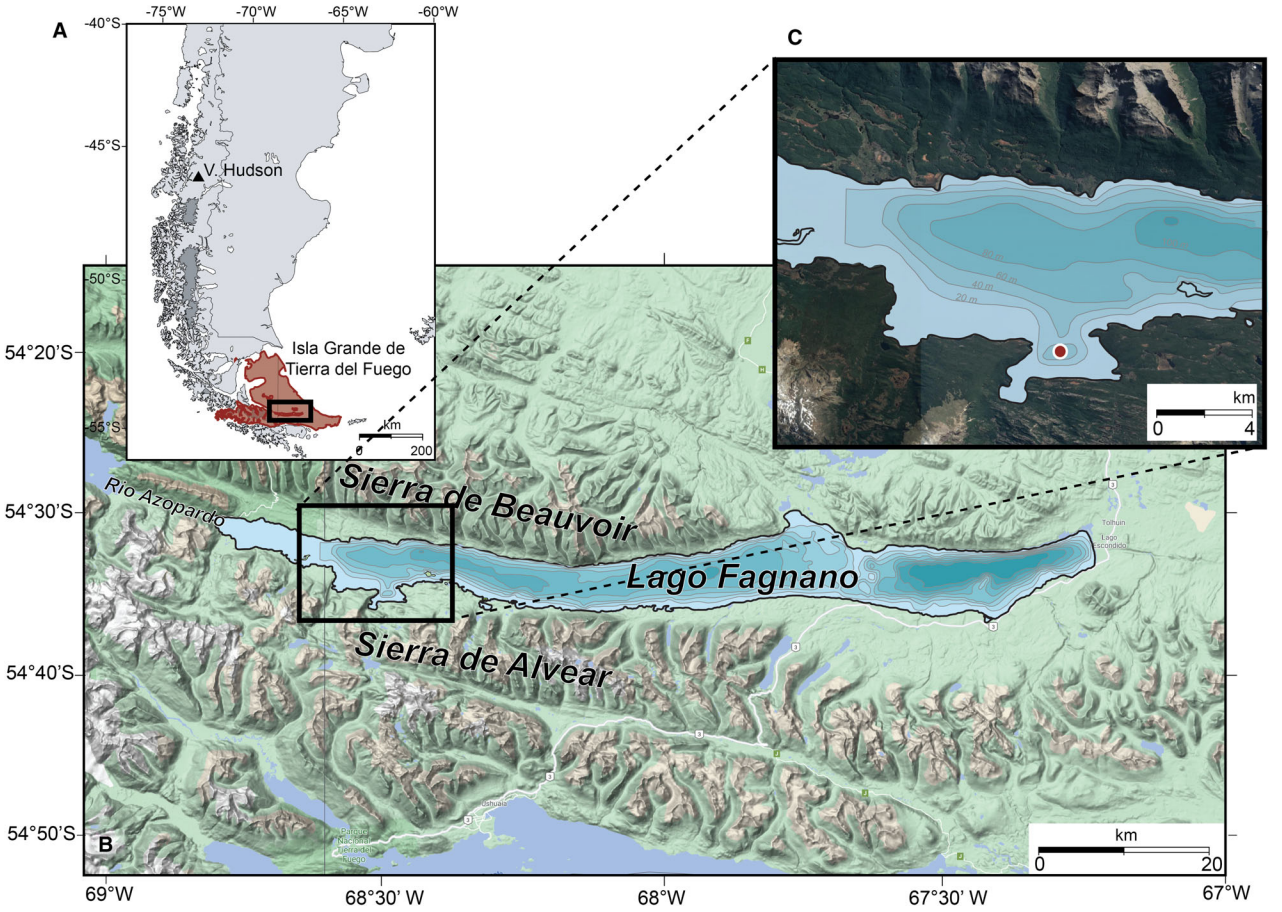

Fig. 1. A. Map of southern South America, indicating in red Isla Grande de Tierra del Fuego and, panel B in black. B. Terrain map indicating with a red dot the position of the piston core LF06-PC8 from Bahia Grande. Google Maps (accessed 17 October 2020). C. Satellite image of Bahia Grande and surroundings superimposed by the bathymetry. The red dot indicates the location of core LF06-PC8. Image taken from Google Earth (accessed 10 February 2022, with images acquired on 4 February 2015 by CNES/Airbus Maxar Technologies).

geomorphology (Mercer 1976; Rabassa & Clapperton 1990; Coronato *et al.* 2009), pollen (Musotto *et al.* 2017; Navatini *et al.* 2019), charcoal analyses (Huber *et al.* 2004; Mansilla *et al.* 2016), dendrochronology (Aravena *et al.* 2002; Masiokas & Villalba 2004) and multiproxy sediment records (Rogers & van Loon 1982; Ariztegui *et al.* 2007; Moy *et al.* 2008, 2011; Borromei *et al.* 2010; Lamy *et al.* 2010; Waldmann *et al.* 2010; Kilian & Lamy 2012; van Daele *et al.* 2016; Quade & Kaplan 2017; Zolitschka *et al.* 2019). These palaeoclimate reconstructions reveal apparently contradictory data and regional syntheses remain controversial (Kilian & Lamy 2012).

The high-resolution millimetric-scale geochemical study presented by Neugebauer *et al.* (2022) demonstrates that the lamination observed at Lago Fagnano is associated with Fe and Mn enrichments that can be explained as lacustrine bottom-water redox variations. In our study, we aim a step further, to provide a comprehensive conceptual model relating the lake redox changes to the SHWW, their evolution and frequencies at a high-resolution scale in this area. Therefore, our goal is to infer the possible relation between climate and laminae formation in Lago Fagnano (Fig. 1).

Study area

Tierra del Fuego is an archipelago at the southernmost tip of South America between Chile and Argentina, separated from the mainland by the Strait of Magellan. The archipelago consists of Isla Grande de Tierra del Fuego (also called Tierra del Fuego) and many islands and islets. This archipelago is influenced by volcanic and seismic activity related to the South American and Scotia–Antarctic plate boundaries (Klepeis 1994). One of its most prominent features is Lago Fagnano (known in Chile as Lago Cami), located at 26 m a.s.l. It is 100 km long and 5–15 km wide, trending east–west and traversing Isla Grande de Tierra del Fuego at ~54°S/68°W. It is the largest freshwater lake on the island, and is the world's most southerly large lake outside of Antarctica (Herdendorf 1982) (Fig. 1). Lago Fagnano was formed

in the depression created in an asymmetric pull-apart basin within the principal displacement zone of the Magallanes–Fagnano fault system, which is part of the diffuse left-lateral plate boundary (Onorato *et al.* 2021). The strike-slip rate along this boundary is approximately 6.6±1.3 mm a^{-1} (Smalley *et al.* 2003). The most severe earthquake measured in Tierra del Fuego (M 7.8) occurred along the eastern end of Lago Fagnano in 1949 (Pedrera *et al.* 2014).

Lago Fagnano is divided into two main sub-basins (230 m in the east and 180 m deep in the west; Waldmann *et al.* 2008). The outflow connecting Lago Fagnano to the Pacific Ocean is Rio Azopardo, via the Whiteside Channel and the Strait of Magellan. The lake water residence time is about 20 years, based on a lake volume of 43 km^3. Lago Fagnano is an oligotrophic lake (Mariazzi *et al.* 1987; Ritcher *et al.* 2010). Its main source of water is precipitation. However, several small cirque glaciers between 900 and 1300 m a.s.l. supply meltwater, with more significance towards the western part of the lake. The altitude of the present equilibrium line at ca. 1100 m a.s.l. suggests that most of these glaciers are in rapid recession (Coronato *et al.* 2008). Indeed, Bahía Grande also has a small catchment area that supplies sediment directly into it.

The present-day climate is semi-arid and cold (annual average temperature 5.8 °C, precipitation 550 mm; Moy *et al.* 2011). The principal feature of the Fuegian climate is the westerly wind system. Lago Fagnano's location and orientation make this site an excellent location to examine the Holocene variation of the SHWW. The lake runs parallel to the wind field and the upwind cordillera is relatively low in elevation (reaching 2469 m a.s.l. (relative to ~3000 m a.s.l. of the Patagonian Ice Fields) and above 4000 m a.s.l. further north), resulting in a weaker rainshadow effect that supports forests of *Nothofagus pumilio* and *Nothofagus antarctica* (Coronato *et al.* 2009). The westerlies are important throughout the year, but as a general rule the SHWW intensity is stronger in summer (December to February) than in winter (June to August), when the core of the SHHW is displaced northwards (Lamy *et al.* 2010). Precipitation follows wind speed only during the summer months (Garreaud *et al.* 2013). The strength of the westerly winds and surface air temperature (SAT) are positively correlated in winter and inversely correlated in summer (Garreaud *et al.* 2013). At a larger scale, in Patagonia El Niño events are associated with weaker SHWW, whereas during La Niña stronger SHWW occur (Schneider & Gies 2004). Additionally, the SHWW at the latitude of Tierra del Fuego are influenced by the El Niño/Southern Oscillation (ENSO) (Rees *et al.* 2015). Garreaud *et al.* (2013) correlate Tierra del Fuego summer rainfall anomalies with the Antarctic Oscillation and winter anomalies to the strength of the SHWW. Garreaud *et al.* (2013) also observe a positive relation between the SHWW and the SAT in winter. In summer the SHWW and SAT are inversely related.

Material and methods

In this work we focus on the uppermost 185 cm of piston core LF06-PC8 (54°35′26.16″S, 68°29′21.87″W, water depth 69 m; Fig. 2). The core was acquired in 2006 using a Kullenberg-type coring system deployed from a 12 m research vessel, the *R/V Neecho* (Stanford University, USA), from Bahía Grande in Lago Fagnano (Figs 1, 2).

Physical properties and magnetic susceptibility

Immediately after core splitting and surface cleaning, we used the GEOTEK Multi-Sensor Core Logger at ETH Zurich (Switzerland) to take continuous digital photographs of core LF06-PC8, and analysed for magnetic susceptibility (MS) and density at 1-cm spatial resolution. Magnetic susceptibility was additionally re-acquired at a higher resolution (0.5-cm intervals) with a point sensor, on the wet sediment cores after core splitting using the GEOTEK Multi-Sensor Core Logger at the USGS Coastal Marine Geology facility in Menlo Park, CA (USA). Unfortunately, a small section of this core (between 236 and 253 cm) was lost in transfer to the photography laboratory and therefore could not be photographed, creating a noticeable gap in the full core photograph (Fig. 2C).

Organic geochemical analyses

The stable carbon and nitrogen isotopic composition and C and N concentrations of bulk organic matter were derived from 5 ml (wet) samples collected uniformly throughout the core at 1 cm intervals. Brodie *et al.* (2011) report analytical bias in the $\delta^{13}C$ and $\delta^{15}N$ values of bulk organic matter from various acid treatments. As a result, core LF06-PC8 was tested to determine whether the removal of inorganic carbon was necessary (Mucciarone 2021). No discernible difference was found in the carbon concentration between 1 M HCl treated and untreated samples, thus untreated samples were freeze-dried and weighed into tin capsules and analysed on a Carlo Erba NA1500 Series 2 elemental analyser, coupled to a Finnigan Delta Plus isotope ratio mass spectrometer via a Finnigan ConFlo II open split interface, at the Stanford University Stable Isotope Biogeochemistry Laboratory (USA). The results are presented in standard delta notation, with $\delta^{13}C$ reported relative to the VPDB carbonate standard and $\delta^{15}N$ relative to air. We used L-glutamic acid USGS-40 (NIST RM8573) as our standard for calibration, and the precision reached on 102 USGS-40 measurements is ±0.1‰ for $\delta^{15}N$, ±0.08‰ for $\delta^{13}C$, ±0.22% for N and ±0.75% for C weight percent concentrations.

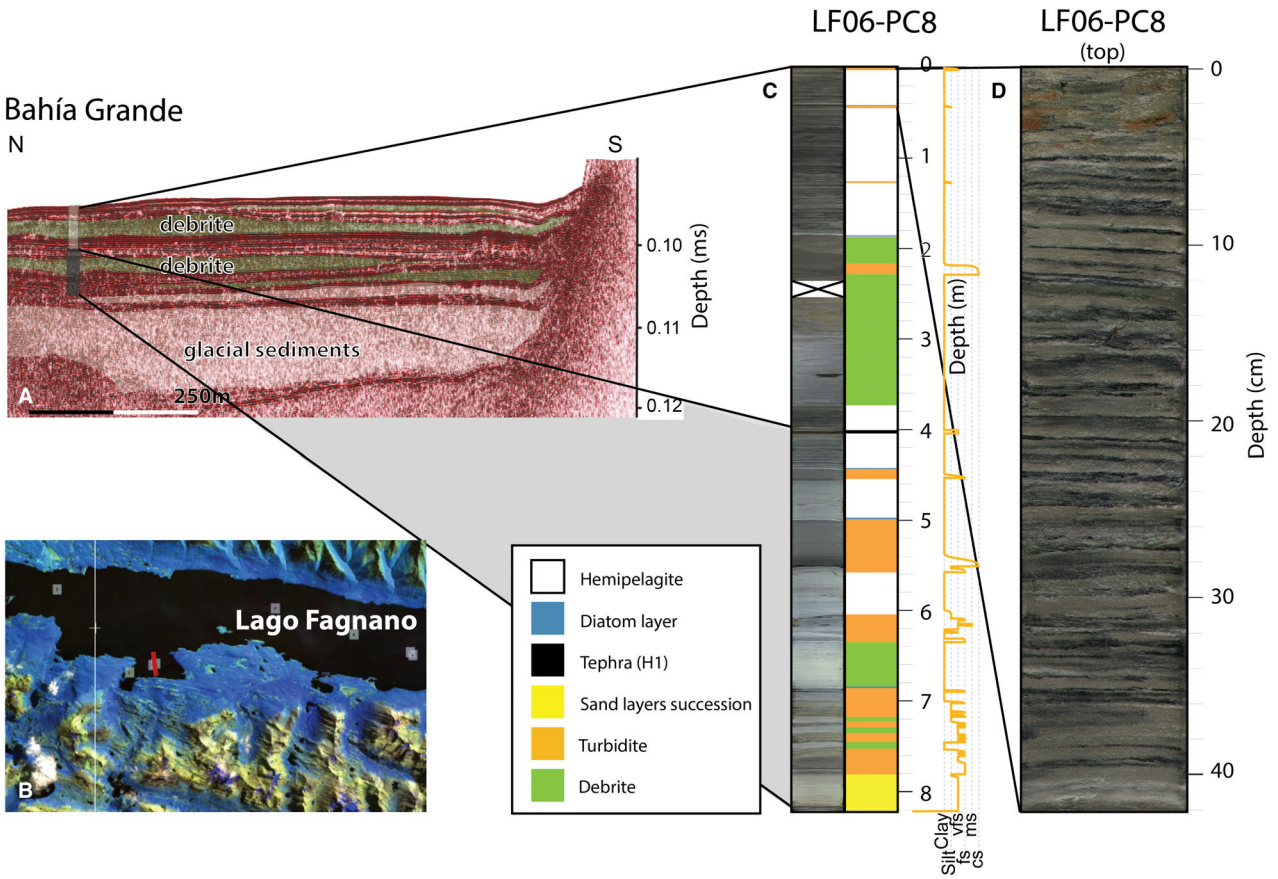

Fig. 2. A. High-resolution seismic profile of Bahía Grande indicating the sediment core and a schematic acoustic facies interpretation. B. False colour satellite image of the western part of Lago Fagnano and Bahía Grande, with a red line indicating the seismic profile (A). C. Image of core LF06-PC8, lithology and visually described grain size (vfs = very find sand; fs = fine sand; ms = medium sand; cs = coarse sand). D. Detailed image of the upper part of core LF06-PC8 with characteristic lamination.

Inorganic geochemical analysis

Major elements were measured using the Avaatech X-ray fluorescence (XRF) core scanner at the Texas A&M IODP (Integrated Ocean Drilling Program) facility (USA) at 2-mm resolution in the laminated sediment intervals and at 5-mm resolution on the debrite intervals. The target elements (Al, Si, S, K, Ca, Ti, Mn, Fe, Ba, Ni, Cu, Br, Rb, Sr and Zr) were measured as counts per second (cps) using X-rays at both 10 and 30 kV. For this study only the elements Al, Ca, Fe, Ti and Mn are represented and interpreted. Data were collected for 40 and 20 s for 2- and 5-mm intervals, respectively. To corroborate the various factors influencing the geochemical composition of the sediment, we conducted principal component analysis (PCA) using the software package PAST version 4.40 (Hammer *et al.* 2001; Fig. 3). The normalized element counts were standardized by subtracting the mean and dividing by the standard deviation (Davis 1986), following Bahr *et al.* (2014). For the PCA we used only those elements with the highest intensities, that is, Al, Si, K, Ca, Ti, Mn, Fe, S and Ba.

The chemical composition of the glass particles of glass (tephra deposit) was determined using a JEOL 8900 electron microprobe with a 15 kV, 10 nA beam, defocused (10 μm) to avoid mobilizing the alkali metals.

Chronology

Dating lacustrine sediments in a cold environment presents a significant challenge owing to the scarcity of carbon suitable for radiocarbon analysis. The chronology for core LF06-PC8 is based on four radiocarbon analyses of wood fragments and bryophytes (Table 1) carried out at the Center for Accelerator Mass Spectrometry at Lawrence Livermore National Laboratory (USA). Calibrated ages were obtained by means of CALIB 8.2 software (Stuiver *et al.* 2021) and the SHcal20 (Hogg *et al.* 2020) calibration curve at the 95% confidence interval. Since dates at depths 228 and 253.5 cm were obtained from turbidite/debrite deposits, they were not used in the age model. An additional age was provided by a tephra layer, identified as Hudson H1 (Stern *et al.* 2016). Therefore, we decided to show all of

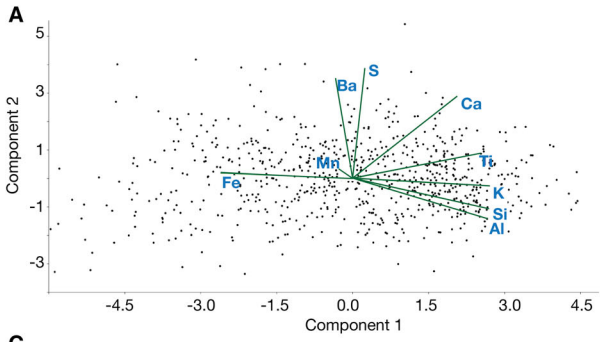

B

PC	Eigenvalue	% variance
1	4.80	53.36
2	1.58	17.59
3	1.16	12.88
4	0.78	8.55
5	0.46	5.06
6	0.13	1.46
7	0.05	0.51
8	0.04	0.42
9	0.02	0.18

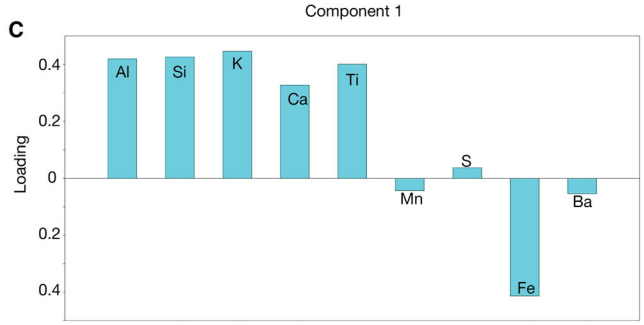

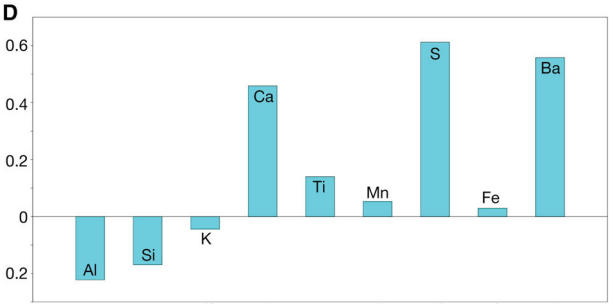

E

	Al	Si	K	Ca	Ti	Mn	S	Fe	Ba
Al		0.000	5.2E-297	1.2E-34	1.0E-98	0.129	0.017	4.4E-199	1.1E-07
Si	0.976		0.0E-01	1.4E-45	4.6E-108	0.024	0.014	1.7E-215	0.837
K	0.910	0.919		3.4E-90	1.6E-208	0.295	0.041	1.4E-228	0.018
Ca	0.436	0.495	0.648		1.7E-159	0.022	4.9E-29	2.5E-66	3.9E-08
Ti	0.669	0.691	0.843	0.784		0.004	0.554	5.78E-130	0.073
Mn	-0.155	-0.168	-0.149	-0.082	-0.102		0.309	1.20E-10	0.029
S	-0.086	-0.088	0.073	0.410	0.144	-0.036		0.878	1.3E-05
Fe	-0.833	-0.850	-0.862	-0.576	-0.735	-0.271	-0.006		0.074
Ba	-0.240	-0.140	-0.170	0.245	-0.064	0.078	0.215	0.064	

Fig. 3. A. Principal component analysis using PAST version 4.40 software (Hammer *et al.* 2001) of XRF data of only the laminated intervals, avoiding turbidites, and the elements Al, Si, K, Ca, Ti, Mn, Fe, S and Ba. B. Table of principal components (PCs), and their eigenvalues and variance. C. Bar chart indicating the values corresponding to PC1, responsible for 53.4% of the variance of XRF data. D. Bar chart indicating the values corresponding to PC2, responsible for 17.6% of the variance of XRF data. E. Correlation matrix with significant positive correlation ($r > 0.60$ and p-value <0.01) between Al, Si, K, Ca, and Ti (green), and significant negative correlation between Fe and the other elements (red) for the laminated sediment intervals.

the data in depth along with the obtained ^{14}C calibrated ages, and to perform a simple linear age model for the uppermost hemipelagite.

Optical microscopy

We undertook microscopic observation of the sediment samples using a petrographic microscope at US Geological Survey, Menlo Park. This method was especially relevant to understanding the biogenic composition of the lighter sediments lying on top of the turbidites. Qualitative observational data helped us to correlate the LF06-PC8 tephra to the H1 event. The andesitic glass exhibits a distinct green/brown tint when observed through a microscope.

Results

Sediment stratigraphy

Six sediment facies characterize core LF06-PC8: hemipelagites, debrites, turbidites, diatom layers, glacio-

Table 1. AMS radiocarbon ages from core LF06-PC8's sedimentary record. Calibrated ages were obtained using Calib 8.2 (Stuiver *et al.* 2021) and the SHCal20 calibration curve (Hogg *et al.* 2020) at 95% confidence intervals. The age of the Hudson H1 tephra represents the mean ^{14}C age determined at various lakes (Stern *et al.* 2016).

AMS laboratory reference	Core depth (cm)	Sample material	Radiocarbon age (a BP±1σ)	Median age (cal. a BP)	2σ range (cal. a BP)
154 730	2.5	Wood	190±30	174	0–283
N92831	136.0	Wood	4135±30	4617	4447–4817
N92832	228.0	Wood	6105±45	6925	6753–7156
N92833	253.5	Bryophytes	6965±40	7757	7671–7917
Hudson 1				8434	8379–8537

lacustrine sediments, and tephra (Fig. 2). The uppermost 185 cm of the succession is dominated by hemipelagic sediments. Below 185 cm, the sediment succession is dominated by very fine to coarse sand turbidites (between 5- and 55-cm thick) and debrites (ranging from a few centimetres to almost 1.5-m thick). Turbidites and debrites generally underlie a grey layer with a high diatom content (microscopic observation; Fig. 2). A tephra deposit is observed at 397.5 cm top and 401.4 cm bottom. The bottommost section corresponds to a succession of millimetric very fine sand layers related to glaciofluvial processes.

Focusing our attention on the core's uppermost 185 cm, we found hemipelagites and turbidities. Hemipelagite facies in Lago Fagnano are characterized by olive and dark olive laminations that exhibit a homogeneous clayey grain size. Thereafter, we considered a lamina to be a pair of olive and dark olive clay sediment layers. The uppermost 185 cm represent the best-preserved record of hemipelagic sediments in the core, and they contain 275 laminae (visual count). The mean thickness of each lamina is ~0.65 cm, and they range from several millimetres to several centimetres (Figs 2, 4, 5). Hemipelagic sediments are characterized by MS values between 2 and 10 SI and densities between 1.2 and 1.35 g cm^{-3}. There are four exceptions at 46, 66, 108 and 112 cm depth, with densities of 1.1, 0.6, 0.6 and 0.9 g cm^{-3}, respectively. Three thin (~2 cm) turbidite deposits interrupt the hemipelagic sedimentation at the core top, at 42 and 127 cm. At 185 cm, a massive (182-cm-thick) multievent debrite divides the sediment core's upper interval, dominated by hemipelagic sediments, from its lower one, dominated by mass transports deposits (Fig. 2). Turbidites are olive-grey clayey to fine sand layers characterized by a fining sequence upwards, sharp bases and density values around 1.5 g cm^{-3} and MS values vary from 5 to 12 SI.

Age model

We analysed four radiocarbon samples to obtain a chronological framework (Table 1). However, only the uppermost two samples, which correspond to pieces of wood deposited within the hemipelagic interval at 2.5 and 136 cm depth (~170 and ~4620 cal. a BP, respectively) were used for the age model, since the lowest two samples were obtained from debrites (Table 1). Finally, at ~400 cm we found a deposit corresponding to the Hudson H1 tephra, whose age and composition are very well constrained in the region (Figs 2 and 6; the mean age of the various lakes is 8434 cal. a BP; Stern *et al.* 2016).

Because of the complexity of the stratigraphy and the lack of datable sediments, we could develop only a basic age model for the core's uppermost 185 cm. Based on our frail or poorly constrained age model, the average rate of hemipelagic sedimentation in the Bahia Grande basin was ~30 cm ka^{-1}, while the rate in the adjacent deep basin of Lago Fagnano was 18 cm ka^{-1} (Moy *et al.* 2011).

Geochemical proxies

Isotopic composition of organic matter. – In core LF06-PC8, hemipelagic sediments show C/N ratios between 8

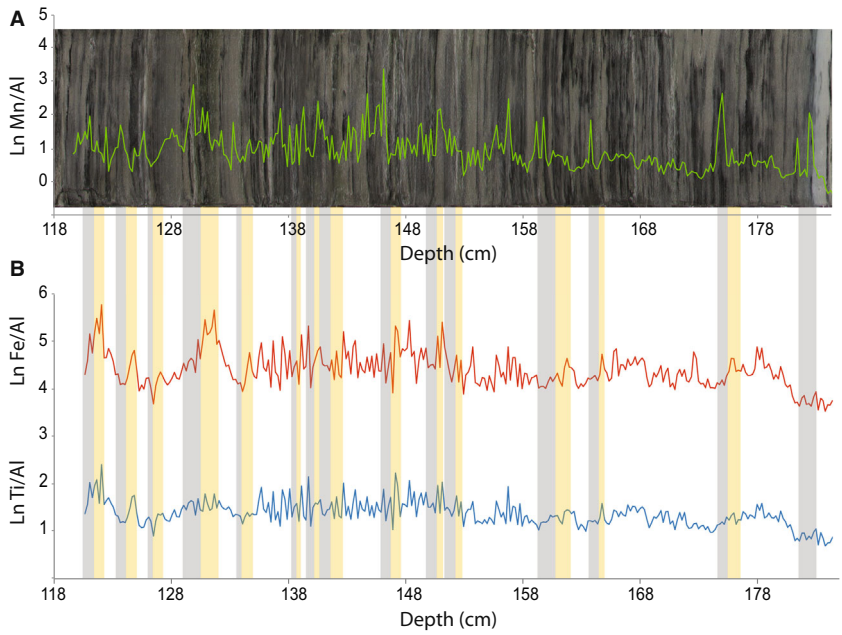

Fig. 4. Scanned image of core LF06-PC8 showing laminations and the greyish diatom layers. A. Ln Mn/Al ratio plotted on the image to illustrate the connections between laminations and geochemistry on a logarithmic scale (Weltje *et al.* 2015). B. Ln Ti/Al and Ln Fe/Al ratios, showing that several enrichments are not overlapped. Colour bars indicate Ln Mn/Al ratio (grey bars) and Ln Fe/Al ratio (orange bars) paired enrichment, interpreted as preserved palaeo-redox fronts.

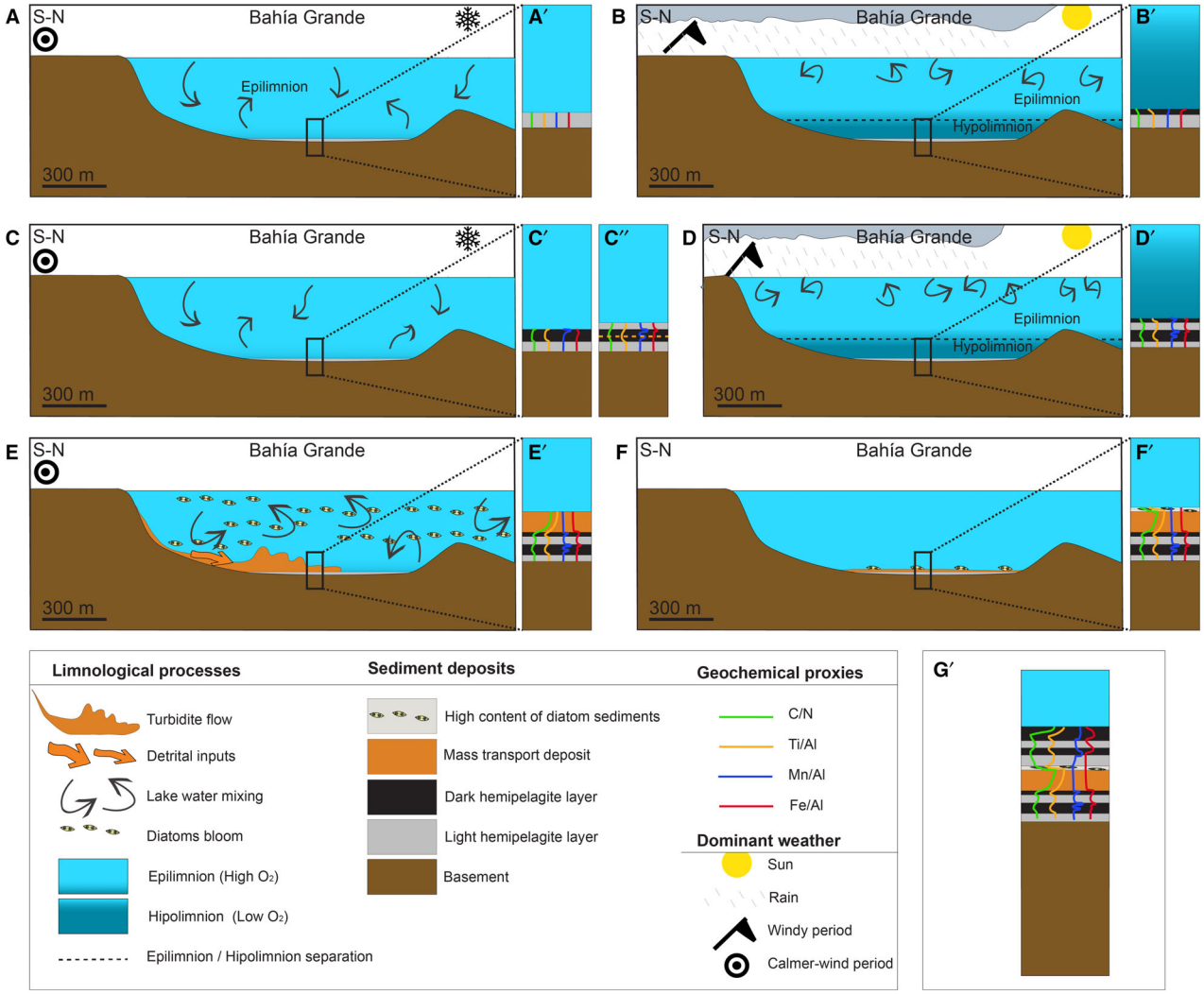

Fig. 5. Progressive cross-sections (south to north) of Bahía Grande in Lago Fagnano, indicating the stages of lamination formation and detailed schemes of chemical reactions at the water–sediment interface. A, A'. Initial stage with mixed and ventilated lake water occurring during winter (low temperatures and low SHWW), and initial conditions of C/N, Ti and Mn/Al. B, B′. Laminae production with dysoxic/anoxic hypolimnion when warm conditions prevail (probably associated with intense SHWW or higher insolation) and decrease in C/N and Ti and certain increases in Mn and Fe. C, C′. Third stage corresponds to a normal winter, with mixed lake water and an absence of hypolimnion, and C/N decreases to similar levels to stage A'. High enrichment in Mn at the boundary between dark and light lamina (see article for details). C″. Eventual persistence of C′ stage conditions. During this stage oxygenated waters originate a redox front. The oxidant front penetrates downwards (dashed orange line), forming the lower Mn/Al peak. D, D′. Similar conditions to (B) stage. E, E′. Mass transport event with higher C/N ratio, as upland plants are contained in the sediment, and higher Ti owing to more terrigenous influence. F, F′. Diatom blooms associated with the increase in nutrients promoted by a mass transport event; the diatom layer has a high Si content.

and 10 (Fig. 7). Light layers have average values of C/N, $\delta^{13}C$, and $\delta^{15}N$ of 10.1±1.7, −25.4±0.6‰, and 2.9±0.5‰, respectively, whereas dark layers have mean values of 9.7±0.6, −25.2±0.3‰, and 3±0.4‰, respectively. Therefore, we did not observe significant differences between the light and dark layers. Turbidites exhibit higher C/N peaks, and the C/N ratios associated with these C/N peaks range from 12 to 20 (Fig. 7). The $\delta^{13}C$ and $\delta^{15}N$ values (−26.0 to −27.5‰ and 1.3 to 2.3‰, respectively) decrease relative to the rest of the sediment facies. This is especially evident in the turbidites at ~44 and ~125 cm (Fig. 7).

Major elements. – The relative abundance of major elements can be used to infer sedimentary processes as well as diagenetic phenomena. We differentiated two groups of major elements. First, Al, Ti and Ca exhibit correlation coefficients close to 1 (Fig. 3), suggesting a relationship between Ca and the detrital fraction, probably caused by low carbonate productivity as observed in other lacustrine systems (Mesa-Fernández *et al.* 2018). The second group, Mn and Fe, relates to redox processes occurring within the sediments rather than with detrital input, in both the lacustrine and marine records (e.g. Davison *et al.* 1982; Naeher *et al.* 2013; Jimenez-

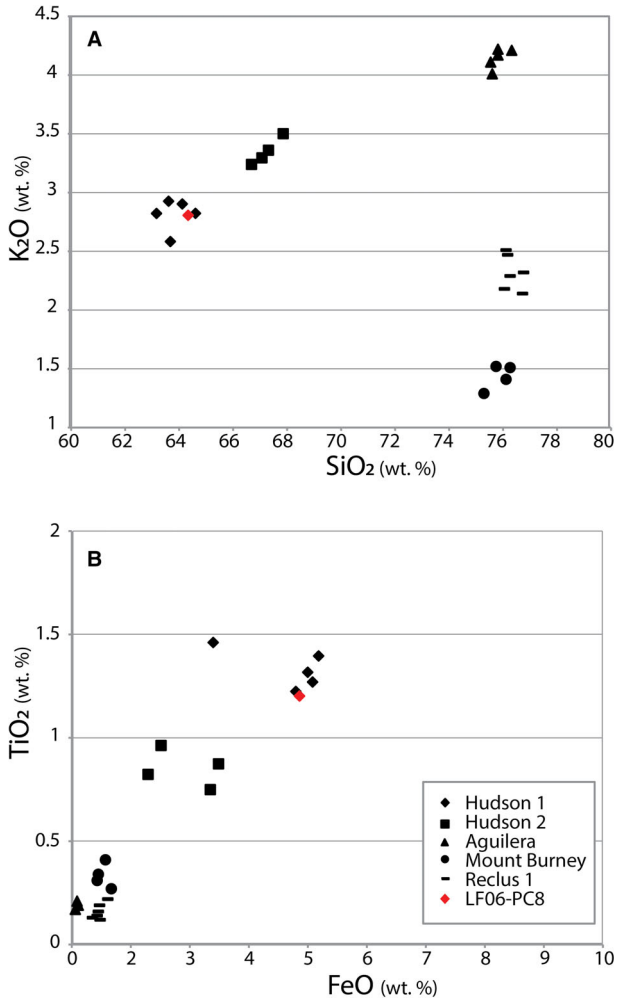

Fig. 6. Elemental composition of glass from major late Quaternary volcanic eruptions of the Andean Volcanic Zone (Naranjo & Stern 1998; Stern 2008). Plot showing the weight percents of: (A) SiO_2 vs. K_2O and (B) TiO_2 and FeO. In red, we show the analysed glass in this study.

Espejo *et al.* 2020). Additionally, we conducted a PCA on the XRF data for only the laminated intervals to obtain a more detailed insight into the main factors governing the elemental composition. The first two principal components (PCs) explain 70.9% of the variance (Fig. 3B). PC1 explains 53.4% of the total variance, showing high scores for Al, Si, K, Ca and Ti, negative for Mn and Ba, and strongly negative for Fe (Fig. 3C). This evidence indicates that the Fe record at Lago Fagnano is not associated with siliciclastic elements but with other mineral phases. Non-detrital Fe-enriched phases are common redox-sensitive minerals, typically pyrite and iron oxides, and their presence is confirmed by previous millimetre-scale studies in this core (Neugebauer *et al.* 2022). PC2 (17.5% of total variance) shows a high score for Ca, S and Ba, slightly positive for Mn and Fe, and negative for Al, Si and K (Fig. 3D). PC2 points again to the lack of covariance between Fe and Mn and detrital elements such as Al and K.

To correct for dilution effects, Mn and Fe concentrations were normalized to Al. This normalization assumes that the Al in sediments is contributed by aluminosilicates (Calvert 1990). Most Mn/Al enrichments are coincident with Fe/Al enrichments (Fig. 4) and commonly found in the transition from dark to light layers or within the thin dark layers between light laminae (Fig. 4).

Tephra analyses. – Core LF06-PC8 contains a tephra at ~400 cm, and in the studied core this level is characterized by the presence of andesitic volcanic glass enriched by FeO and TiO_2 (Fig. 6).

Selected proxies and interpretation

Provenance and delivery mechanisms were inferred using bulk organic matter $\delta^{13}C$ and $\delta^{15}N$ values, as well as elemental data derived from XRF scanning. The C/N ratio is commonly used to differentiate between algal and terrestrial sources of the organic matter in lacustrine sediments (Meyers & Teranes 2001). Terrestrial organic matter derived from vascular land plants typically has C/N atomic ratios greater than 20, whereas lacustrine algae typically have C/N values lower than 10 (Meyers 2003). Because lacustrine organic matter is a mixture of terrestrial and aquatic organic matter, C/N ratios may be used to identify the relative contributions of these two endmembers to the sediment (Meyers & Teranes 2001). Moreover, grain size may exert control on the C/N ratios (Ghazoui *et al.* 2019), and $\delta^{13}C$ and $\delta^{15}N$ can be considered as indicators of productivity (Meyers & Teranes 2001). Nevertheless, it must be noted that the sampling intervals inherent to each of these three methods are different: while $\delta^{13}C$ and $\delta^{15}N$ values (at 1-cm intervals) are useful to identify centennial variation, XRF core-scan data (at 2-mm intervals) potentially provide decadal-scale resolution.

Discussion

This palaeoenvironmental study of Lago Fagnano focused on the uppermost 185 cm of core LF06-PC8, corresponding mostly to hemipelagic sediments.

Sedimentary processes

Tephra and mass transport deposits. – The tephra layer analysed has been geochemically correlated to the major Early Holocene eruption H1 of the Hudson volcano (Table 2, Fig. 6). Glass from the Hudson event is distinct from other large eruptions of the Andean Volcanic Zone as its andesitic composition (rich in FeO and TiO_2) differs from that of the rhyolitic glass associated with other tephra (Fig. 6) (Stern 2008). Glass from the

Hudson 1 tephra is also notable for its relatively high K_2O content (Stern 2008). The Late-Holocene Aguilera tephra is the only regional major Holocene event to contain higher K_2O values.

Turbidites and debrites are sedimentary deposits resulting from rapid and ephemeral mass transport processes (Stow & Zeinab 2020). In the Bahía Grande sediment core's uppermost 185 cm, the only mass transport deposits observed correspond to turbidites exhibiting higher C/N peaks, indicative of terrestrial organic matter (C/N values 12.4±2.5), compared with more 'algal' hemipelagites (9.9±1.1). All turbidites show high C/N ratios and significantly lower $\delta^{13}C$ and $\delta^{15}N$, influenced by organic matter from littoral areas, from the catchment basin or associated with grain size variations described in turbidite layers (Fig. 7). Diatom-rich layers occur above each of the turbidites, probably related to an increase in nutrient availability in the lake water following mass transport events (Mackay *et al.* 1998).

The age of this uppermost turbidite is compatible with the historic 1949 Fagnano earthquake. Situated along an active plate boundary with regular and strong seismic events, earthquakes are a probable trigger mechanism for mass transport episodes (Costa *et al.* 2006; Waldmann *et al.* 2008). The synchroneity found between this turbidite and the seismic record opens the door to more palaeoseismic studies in the region.

Hemipelagic sediments: formation of laminations. – The hemipelagic interval is characterized by conspicuous millimetric lamination of olive and dark olive clays. In core LF06-PC8 we inferred an algal origin for the organic matter in the hemipelagic facies, based on its C/N ratio (Fig. 7), but we did not observe this distinction between darker and lighter levels. However, since the isotopic composition between light and dark layers is highly homogeneous, we used XRF data to characterize the hemipelagic deposits and to describe the laminations. Al, Ti, and Ca variability exhibit high correlation coefficients between each other (Fig. 3), but the Ti/Al ratio shows a weak relationship to the dark/light laminations (Fig. 4). In contrast, Mn and Fe are enriched in the dark laminae (Fig. 4). Most Mn/Al enrichments are coincident with Fe/Al enrichments (Fig. 4) and commonly occur at the transition between dark to light layers or in thin dark layers between light laminae (Fig. 4; Neugebauer *et al.* 2022). Also, conspicuous differences are discernible with depth regarding the content of Mn and Fe at the transitions between a dark and a light layer. Such Mn–Fe oxides typically reflect past lake hypolimnic redox conditions (Davison *et al.* 1982; Eusterhues *et al.* 2005; Rush 2010; Kasper *et al.* 2013; Dräger *et al.* 2019).

Reactive Mn is delivered to the lake by rainfall and also by diffusion from coastal sediments. In addition, dissolved Mn^{+2} is present in aquatic systems in low concentrations. However, changes in redox conditions led to a change in dissolved manganese (Mn^{2+}) and iron (Fe^{2+}) content within the water column and/or pore waters, with consequent precipitation of Fe and Mn oxides (Fig. 5C′; e.g. Schaller & Wehrli 1997; Pakhomova *et al.* 2007). Similar models have been proposed for other lakes (e.g. Schaller & Wehrli 1997; Haberzettl *et al.* 2006). In thick dark laminae the Mn/Al enrichments often exhibit double peaks (Fig. 5A). This pattern can be explained by a redox front associated with better-ventilated deep water entering the basin after sediments have been deposited under less well-ventilated conditions (Fig. 5C; Rutten *et al.* 1999; Mangini *et al.* 2001).

The distribution of Mn and Fe within the laminated sediment succession can be explained by episodic anoxic/oxic hypolimnion changes (Fig. 5), as described for other lakes worldwide (Dean 1997; Dräger *et al.* 2019). Low levels of primary production in Lago Fagnano and/or poor organic matter preservation (Mucciarone 2021) suggest that these variations cannot be explained by biological processes alone. Rather, they are best explained by periodic oxygenation of the hypolimnion responding to energetic water column mixing and associated deep lake ventilation (Neugebauer *et al.* 2022). The same link between Mn variations and water oxygenation has been described for another Patagonian lake (Jouve *et al.* 2013) as well as for lacustrine (Schaller *et al.* 1997; Eusterhues *et al.* 2005; Rush 2010; Naeher *et al.* 2013; Dräger *et al.* 2019) and marine environments (e.g. Löwemark *et al.* 2008; De Lange *et al.* 2008; Jimenez-Espejo *et al.* 2020). This differential variation in Mn and Fe preservation within a lacustrine basin has been described in other regions and linked to variations in local conditions and sedimentation rates (e.g. Granina *et al.* 2004).

Taken together, the geochemical data indicate that laminations in the upper sediment column of Lago Fagnano result from the presence of a variable redox boundary within the water column. In lacustrine systems such redox boundaries are typically associated with incomplete water column mixing and consequent hypolimnetic anoxia/dysoxia (e.g. Naeher *et al.* 2013; Dräger *et al.* 2019). In lakes such as Lago Fagnano, water column mixing is caused by a number of processes, such as wind-generated wave forcing and cooling. The sediments forming under these well-oxygenated conditions are light in colour. In contrast, dark laminae are indicative of poor ventilation. These laminations are probably controlled by winter climatic conditions, yet warmer and calmer periods during summers might also generate water column stratification and increase biological production, a model similar to other locations (e.g. Davies *et al.* 2004; Naeher *et al.* 2013; Makri *et al.* 2021). We note that the presence of persistently stratified conditions has not been described in the few water column studies conducted at Lago Fagnano (Mariazzi *et al.* 1987). To test our interpretation of laminae origin related to winter climatic conditions, a

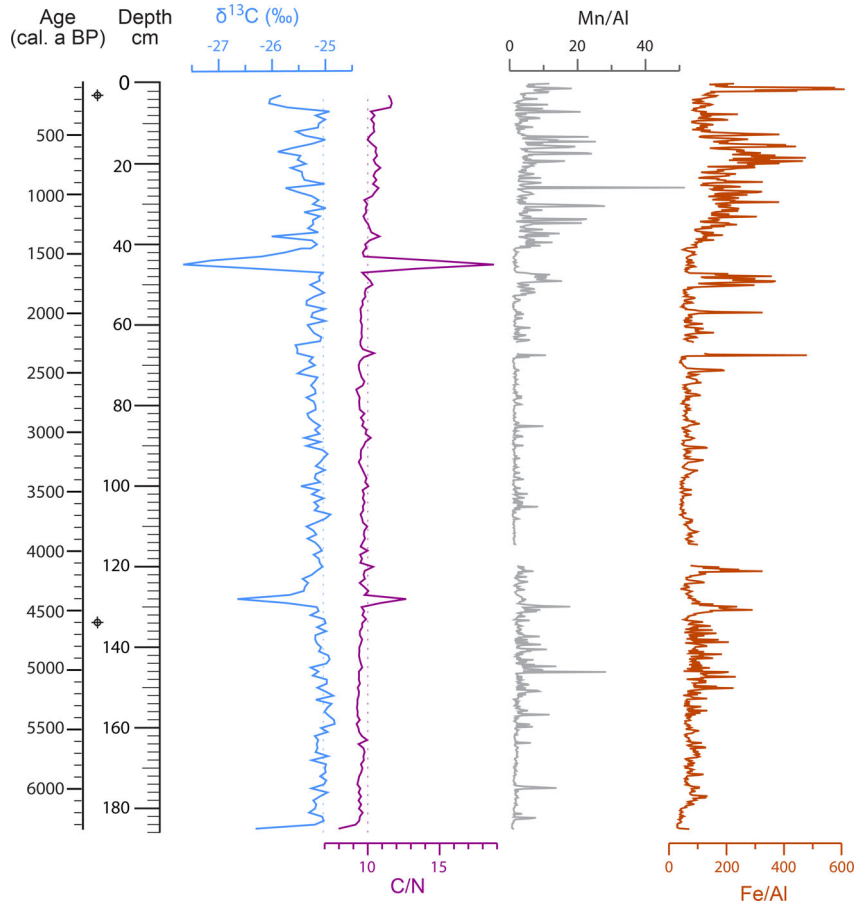

Fig. 7. Core LF06-PC8 log, showing bulk major element ratios Mn/Al (orange), Fe/Al (brown), organic matter $\delta^{13}C$ (blue), and C/N (purple) vs. age (cal. a BP) and depth (cm). The left side indicates the core LF06-PC8 age model tie points and climate periods described for the study region.

seasonal and multiannual lake monitoring programme is needed to examine the epilimnion and hypolimnion at Bahia Grande in Lago Fagnano.

Laminations: cyclicity and triggering process

Even though our age model has limitations, we infer an average periodicity of ~22 years for pairs of laminae (light–dark) during the last ~6.3 ka (275 laminae in ~6130 years, corresponding to the first ~185 cm of hemipelagic sedimentation), as described above. These bidecadal quasicycles have a period coinciding with that of the Hale solar cycle (Raspopov *et al.* 2004) that is supposed to exert an influence on ENSO events (Landscheidt 2000; Leamon *et al.* 2021). In addition, this cycle may be a subharmonic of the releant 200–250 year periodicity pervasive in the southern hemisphere climate, described at Lago Cipreses (SW Patagonia; Moreno *et al.* 2014), the Falkland Islands (Patagonia Atlantic; Turney *et al.* 2016), and Lago Hambre (southern Patagonia; Pérez-Rodriguez *et al.* 2016), linked to solar influence and the strength of the SHWW.

Variations in water stratification, the formation of a hypolimnion and subsequent generation of sedimentary

Table 2. Geochemical composition of the tephra layer found in core LF06-PC8, identified as Hudson Eruption H1 at 397.5–401.4 cm depth.

	Na_2O	MgO	Al_2O_3	SiO_2	K_2O	CaO	TiO_2	MnO	FeO	Total
Mean	5.812	1.407	16.031	63.165	2.755	2.904	1.180	0.159	4.771	98.186
Standard deviation	0.274	0.097	0.165	0.657	0.189	0.157	0.072	0.018	0.184	0.533
Range	0.860	0.321	0.684	2.168	0.725	0.445	0.244	0.068	0.632	1.859
Minimum	5.415	1.243	15.721	62.043	2.224	2.687	1.055	0.125	4.429	97.318
Maximum	6.275	1.564	16.405	64.211	2.949	3.132	1.299	0.193	5.061	99.177
Count	13	13	13	13	13	13	13	13	13	13
confidence level (95.0%)	0.166	0.058	0.100	0.397	0.114	0.095	0.044	0.011	0.111	0.322
Normalized	5.92	1.43	16.33	64.33	2.81	2.96	1.20	0.16	4.86	100.00

laminations probably reflect changes in lake water temperature and regional wind intensity in austral winters (Fig. 5). No data to evaluate the role of temperature and precipitation in controlling water column dynamics are available from Lago Fagnano. However, temperature and winds usually play a crucial role in great lake hypoxia (e.g. Rowe *et al.* 2019). Indeed, while wind is a frequent phenomenon in the Lago Fagnano area, ventilation triggered by the SHWW might be active throughout the year, not only on a bi-decadal basis. In contrast, water mixing owing to the thermobaric instability of Lago Fagnano would happen eventually in winter if conditions were optimal (with surface waters reaching the 4 °C density maximum), allowing overturning of the water column (Weiss *et al.* 1991; Piccolroaz & Toffolon 2013), and might be the most likely mechanism in a large lake at this latitude. Moreover, in winter the westerlies are positively correlated with the SAT, whereas in summer the relation between the SAT and winds is negative (Garreaud *et al.* 2013). It is also known that in southern Patagonia the El Niño periods are associated with weaker SHWW, colder and with less precipitation than the La Niña intervals (Schneider & Geis 2004). From the results presented here, we believe that ENSO-like variability may be relevant for explaining the origin of sediment laminations (e.g. Fischer & Bottjer 1991; Ripepe *et al.* 1991; Damnati & Taieb 1995; Muñoz *et al.* 2002). La Niña would be associated with mild winters with strong SHWW, in which lacustrine stratification may persist throughout the year, allowing dark laminae deposition (Fig. 5B). In contrast, colder winters with weaker SHWW during El Niño-like conditions may force the intensification of water column ventilation (Fig. 5C).

Garreaud *et al.* (2013) also find seasonal differences in southern Patagonia. Whereas winter precipitation anomalies relate to the SHWW, summer anomalies are linked to the Antarctic Oscillation. Warmer summers are characterized by a significant weakening of the SHWW and an increase in temperature, which in turn can promote productivity and ultimately strengthen the lamination effect. This interpretation is in agreement with other studies in south-eastern Patagonia, which highlight the role of the SHWW in controlling lacustrine sedimentary processes (Zolitschka *et al.* 2019). If our hypothesis is correct the Lago Fagnano data are a rare, sensitive record of the SHWW at decadal resolution and, if new dating methods are applied, offer a major opportunity for future SHWW reconstructions.

Palaeoclimate reconstruction

The Holocene palaeoclimate in southern South America is a matter of debate, as records often show great site-to-site differences (Kilian & Lamy 2012; Bertrand *et al.* 2017; Zolitschka *et al.* 2019). This variability can be associated with the interaction between the SHWW and the Andes, which produces enhanced rainfall west of the Cordillera and a rainshadow effect to the east, creating a strong west–east rainfall gradient.

The most characteristic feature of the sediment record from Lago Fagnano is the bidecadal laminations occurring throughout the last ~6.3 ka, probably owing to water ventilation. Although our records display limitations to obtaining a detailed palaeoclimate reconstruction, owing to the frail or poorly constrained age model, we can still infer some general features. Firstly, the described Lago Fagnano bidecal laminations are coherent as a subharmonic of the described 250-year periodicity associated with the SHWW in locations such as the Falkland Islands (Turney *et al.* 2016), triggered by solar variations. Additionally, the process generating the lamination has persisted for the last ~6.3 ka (Fig. 7), yet the lamination pattern, variability and intensity have not been constant. From ~6 to ~2 cal. ka BP the Mn/Al and Fe/Al enrichments were less intense and variable (Fig. 7). These low Ln Mn/Al and Ln Fe/Al ratios may relate to diagenesis or be in response to palaeoenvironmental conditions. Diagenesis could have promoted dissolution of Fe–Mn oxides in pore-waters, but lower Mn and Fe precipitation could also be associated with less intense ventilation changes in Lago Fagnano and, eventually, with less intense water column stratification and reduced SHWW and/or insolation, thus colder winter temperatures. In our records, the last ~2 ka are associated with higher values of Fe/Al and Mn/Al ratios (Fig. 7), which might reflect more robust water column stratification and correspondingly decreased bottom oxygenation. Detrital input (Ti) also shows higher variability during this period, which could be linked to higher rainfall input (Fig. 7). These conditions are ultimately compatible with an intensification of ENSO activity, as indicated by marked variation in wind and precipitation, in Lago Fagnano driving changes in water column stratification. These results are in agreement with studies that indicate a major climate change in these southern latitudes during the past two millennia, interpreted as a co-intensification of ENSO events in the Western Antarctic Peninsula (Etourneau *et al.* 2013) and other regions in South America (Conroy *et al.* 2008; Makou *et al.* 2010; Fiers *et al.* 2019; Cai *et al.* 2020), as well as SHWW intensification and increased aridity in the northern Tierra del Fuego steppe (Laprida *et al.* 2021).

Conclusions

This study focused on the 1.85-m-long laminated section of a Lago Fagnano sediment core that corresponds to the past ~6.3 ka and its hemipelagic sediments, which preserve palaeoenvironmental and palaeoclimate signals. The hemipelagic sedimentation presents three thin intercalated turbidites. The turbidites are overlain by a grey layer with a high diatom content, reflecting a rapidly

increased nutrient load in the lake and high productivity, associated with mass transport events. Hemipelagites in Lago Fagnano are characterized by laminations composed of paired dark and light layers. The mean recurrence interval of the laminations is estimated to be ~22 years, based on a visual count (275 laminae in ~6120 years). While it may well be fortuitous, this average time step is equivalent to the duration of the modern Hale solar cycle, which might influence ENSO characteristics (the harmonic of the relevant 200–250 year periodicity pervasive in the southern hemisphere climate), linked with solar influence and the strength of the SHWW.

We propose a conceptual model for laminae formation that invokes the existence of a variable redox boundary in deep water. An inferred anoxic/dysoxic hypolimnion produces dark laminae when present, and light laminae when not. At least in Bahia Grande (Lago Fagnano), we suggest that water column mixing is probably forced by thermobaric instability during colder winters. Cold winters can be linked to weaker SHWW during El Niño-like conditions. Therefore, the cooling conditions in winter might promote and intensify ventilation of the water column and produce lighter laminations. In contrast, La Niña-like conditions and/or higher insolation relate to windier and warmer winters, which preserve water stratification throughout the year and produce dark hemipelagite layers.

Based on geochemical ratio variation, this study distinguishes two climate periods. From ~6 to ~2 cal. ka BP Mn/Al and Fe/Al enrichments could relate to greater ventilation of Lago Fagnano, ultimately associated with less stable water column stratification and reduced SHWW and/or insolation, and thus colder winter temperatures. During the last ~2 ka the Fe/Al and Mn/Al ratios and detrital input demonstrate greater variation, which can be interpreted as more robust water column stratification, and this is compatible with an intensification of ENSO activity.

Acknowledgements. – The research has been supported by the Beatriu de Pinós postdoctoral programme at Agència de Gestió Acadèmica i Universitària at Generalitat de Catalunya, NSF grants ATM-0408668 and EAR-1103550 to R. Dunbar, and the Spanish Ministry of Science and Innovation (grant CTM2017-89711-C2-1-P), co-funded by the European Union through FEDER funds. A. García-Alix was also supported by Ramón y Cajal Fellowship RYC-2015-18966 of the Spanish Government (Ministerio de Economía y Competividad). We specially thank Dr. David Wahl (USGS) for his contribution to the development of this article and the tephra analysis and observations. We thank Dr Lysanna Anderson (USGS), Dr Brian Edwards (USGS) and Dr Thomas Gorgas (IODP-TAMU) for their help with the core logger in carrying out the analyses on the cores. We thank Dr Carlota Escutia for her support. We also wish to show our deep gratitude to the reviewers of this article, who helped us to strengthen our study. The authors have no conflicts of interest to declare. All co-authors have seen and agreed with the contents of the final draft, and there is no financial interest to report. We thank the editor and the three referees (Prof. Philip Meyers and two anonymous) for their valuable reviews and suggestions.

Author contributions. – RBD, DM and AVM outlined the design of the study. RBD acquired the grants funding the transport of *R/V Neecho* to Argentina, acquisition and analyses. DA conducted the fieldwork. AVM performed radiocarbon sample preparation and analyses, XRF scans, stable isotopes and physical properties. DM and AVM interpreted the stable isotopes. FJJE interpreted the XRF data on the hemipelagic sediments. FJJE, AGA and IN provided key interpretations in the geochemical model. AGA and AVM created the age model. AVM and FJJE wrote the text, which was edited and reviewed by all of the authors (RBD, DW, DM, AGA, IN and DA).

Data availability statement. – The datasets that support this study are available at Pangaea database.

References

Aravena, J. C., Lara, A., Wolodarsky-Franke, A., Villalba, R. & Cuq, E. 2002: Tree-ring growth patterns and temperature reconstruction from Nothofagus pumilio (Fagaceae) forests at the upper tree line of southern Chilean Patagonia. *Revista Chilena de Historia Natural 75*, 361–376.

Ariztegui, D., Bosch, P. & Davaud, E. 2007: Dominant ENSO frequencies during the Little Ice Age in Northern Patagonia: the varved record of proglacial Lago Frias, Argentina. *Quaternary International 161*, 46–55.

Bahr, A., Jiménez-Espejo, F. J., Kolasinac, N., Grunert, P., Hernández-Molina, F. J., Röhl, U., Voelker, A. H. L., Escutia, C., Stow, D. A. V., Hodell, D. & Alvarez-Zarikian, C. A. 2014: Deciphering bottom current velocity and paleoclimate signals from contourite deposits in the Gulf of Cádiz during the last 140 ka: An inorganic geochemical approach. *Geochemistry, Geophysics, Geosystems 15*, 3145–3160.

Bertrand, S., Lange, C. B., Pantoja, S., Hughen, K., Van Tornhout, E. & Smith Wellner, J. 2017: Postglacial fluctuations of Cordillera Darwin glaciers (southernmost Patagonia) reconstructed from Almirantazgo fjord sediments. *Quaternary Science Reviews 177*, 265–275.

Borromei, A. M., Coronato, A., Franzén, L. G., Ponce, J. F., Sáez, J. A. L., Maidana, N., Rabassa, J. & Candel, M. S. 2010: Multiproxy record of Holocene paleoenvironmental change, Tierra del Fuego, Argentina. *Palaeogeography, Palaeoclimatology, Palaeoecology 286*, 1–16.

Brodie, C. R., Casford, J. S. L., Lloyd, J. M., Leng, M. J., Heaton, T. H. E., Kendrick, C. P. & Yongqiang, Z. 2011: Evidence for bias in C/N, $\delta^{13}C$ and $\delta^{15}N$ values of bulk organic matter, and on environmental interpretation, from a lake sedimentary sequence by pre-analysis acid treatment methods. *Quaternary Science Reviews 30*, 3076–3087.

Cai, W., McPhaden, M. J., Grimm, A. M., Rodrigues, R. R., Taschetto, A. S., Garreaud, R. D., Dewitte, B., Poveda, G., Ham, Y.-G., Santoso, A., Ng, B., Anderson, W., Wang, G., Geng, T., Jo, H.-S., Marengo, J. A., Alves, L. M., Osman, M., Li, S., Wu, L., Karamperidou, C., Takahashi, K. & Vera, C. 2020: Climate impacts of the El Niño–Southern Oscillation on South America. *Nature Reviews Earth & Environment 1*, 215–231.

Calvert, S. 1990: Geochemistry and origin of the Holocene sapropel in the Black Sea. *In* Ittekkot, V., Kempe, S., Michaelis, W. & Spitzy, A. (eds.): *Facets of Modern Biogeochemistry*, 326–352. Springer-Verlag, Berlin.

Canadell, J. G., Le Quéré, C., Raupach, M. R., Field, C. B., Buitenhuis, E. T., Ciais, P., Conway, T. J., Gillett, N. P., Houghton, R. & Marland, G. 2007: Contributions to accelerating atmospheric CO_2 growth from economic activity, carbon intensity, and efficiency of natural sinks. *PNAS 104*, 18866–18870.

Conroy, J. L., Overpeck, J. T., Cole, J. E., Shanahan, T. M. & Steinitz-Kannan, M. 2008: Holocene changes in eastern tropical Pacific climate inferred from a Galápagos lake sediment record. *Quaternary Science Reviews 27*, 1166–1180.

Coronato, A. M. J., Coronato, F., Mazzoni, E. & Vázquez, M. 2008: The physical geography of Patagonia and Tierra del Fuego. *Developments in Quaternary Sciences 11*, 13–55.

Coronato, A., Seppälä, M., Ponce, J. F. & Rabassa, J. 2009: Glacial geomorphology of the Pleistocene Lake Fagnano ice lobe, Tierra del Fuego, southern South America. *Geomorphology 112*, 67–81.

Costa, C., Smalley, R., Jr., Schwartz, D., Stenner, H., Ellis, M., Ahumada, E. & Velasco, M. 2006: Paleoseismic observations of an onshore transform boundary: the Magallanes-Fagnano fault, Tierra del Fuego Argentina. *Revista de la Asocicación Geológica Argentina 61*, 647–657.

van Daele, M., Bertrand, S., Meyer, I., Moernaut, J., Vandoorne, W., Siani, G., Tanghe, N., Ghazoui, Z., Pino, M., Urrutia, R. & De Batist, M. 2016: Late Quaternary evolution of Lago Castor (Chile, 45.6°S): timing of the deglaciation in northern Patagonia and evolution of the southern westerlies during the last 17 ka. *Quaternary Science Reviews 133*, 130–146.

Damnati, B. & Taieb, M. 1995: Solar and ENSO signatures in laminated deposits from Lake Magadi (Kenya) during the Pleistocene/Holocene transition. *Journal of African Earth Sciences 21*, 373–382.

Davis, J. C. 1986: *Statistics and Data Analysis in Geology*. 646 pp. John Wiley, New York.

Davies, J.-M., Nowlin, W. H. & Mazumder, A. 2004: Variation in temporal [^{14}C] plankton photosynthesis among warm monomictic lakes of coastal British Columbia. *Journal of Plankton Research 26*, 763–778.

Davison, W., Woof, C. & Rigg, E. 1982: The dynamics of iron and manganese in a seasonally anoxic lake: direct measurement of fluxes using sediment traps. *Limnology and Oceanography 27*, 987–1003.

De Lange, G. J., Thomson, J., Reitz, A., Slomp, C. P., Principato, M. S., Erba, E. & Corselli, C. 2008: Synchronous basin-wide formation and redox-controlled preservation of a Mediterranean sapropel. *Nature Geoscience 1*, 606–610.

Dean, W. E. 1997: Rates, timing, and cyclicity of Holocene eolian activity in north-central United States: evidence from varved lake sediments. *Geology 25*, 331–334.

Dräger, N., Plessen, B., Kienel, U., Słowinski, M., Ramish, A., Tjallingii, R., Pinkerneil, S. & Brauer, A. 2019: Hypolimnetic oxygen conditions influence varve preservation and d^{13}C of sediment organic matter in Lake Tiefer See, NE Germany. *Journal of Paleolimnology 62*, 181–194.

Etourneau, J., Collins, L. G., Willmott, V., Kim, J. H., Barbara, L., Leventer, A., Schouten, S., Sinninghe Damsté, J. S., Bianchini, A., Klein, V., Crosta, X. & Massé, G. 2013: Holocene climate variations in the western Antarctic Peninsula. *Climate of the Past 9*, 1–41.

Eusterhues, K., Heinrichs, H. & Schneider, J. 2005: Geochemical response on redox fluctuations in Holocene lake sediments, Lake Steisslingen, Southern Germany. *Chemical Geology 222*, 1–22.

Fiers, G., Bertrand, S., Van Daele, M., Granon, E., Reid, B., Vandoorme, W. & De Batist, M. 2019: Hydroclimate variability of northern Chilean Patagonia during the last 20 ka inferred from the bulk organic geochemistry of Lago Castor sediments (45°S). *Quaternary Science Reviews 204*, 105–118.

Fischer, A. G. & Bottjer, D. J. 1991: Orbital forcing and sedimentary sequences. *Journal of Sedimentary Petrology 61*, 1063–1069.

Garreaud, R. D. 2007: Precipitation and circulation covariability in the extratropics. *Journal of Climate 20*, 4789–4797.

Garreaud, R., Lopez, P., Minvielle, M. & Rojas, M. 2013: Large scale control on the Patagonia climate. *Journal of Climate 26*, 215–230.

Ghazoui, Z., Bertrand, S., Vanneste, K., Yokoyama, Y., Nomade, J., Gajurel, A. P. & van der Beek, P. A. 2019: Potentially large post-1505 AD earthquakes in western Nepal revealed by a lake sediment record. *Nature Communications 10*, 2258, https://doi.org/10.1038/s41467-019-10093-4.

Google Maps 2020: *Southern Tierra del Fuego*. Google Maps (online) (accessed 17 October 2020).

Granina, L., Müller, B. & Wehrli, B. 2004: Origin and dynamics of Fe and Mn sedimentary layers in Lake Baikal. *Chemical Geology 205*, 55–72.

Haberzettl, T., Wille, M., Fey, M., Janssen, S., Lücke, A., Mayr, C., Ohlendorf, C., Schäbitz, F., Schleser, G. H. & Zolitschka, B. 2006: Environmental change and fire history of southern Patagonia (Argentina) during the last five centuries. *Quaternary International 158*, 72–82.

Hammer, Ø., Harper, D. A. T. & Ryan, P. D. 2001: PAST: Paleontological statistics software package for education and data analysis. *Palaeontologia Electronica 4*, 1–9.

Herdendorf, C. E. 1982: Large lakes of the world. *Journal of Great Lakes Research 8*, 379–412.

Hogg, A. G., Heaton, T. J., Hua, Q., Palmer, J. G., Turney, C. S. M., Southon, J., Bayliss, A., Blackwe Boswijk, G., Bronk Ramsey, C., Pearson, C., Petchey, F., Reimer, P., Reimer, R. & Wacker, L. 2020: SHCal20 Southern Hemisphere calibration, 0-55,000 years cal BP. *Radiocarbon 62*, 759–778.

Huber, U. M., Markgraf, V. & Schäbitz, F. 2004: Geographical and temporal trends in Late Quaternary fire histories of Fuego-Patagonia, South America. *Quaternary Science Reviews 23*, 1079–1097.

Ito, T., Woloszyn, M. & Mazloff, M. 2010: Anthropogenic carbon dioxide transport in the Southern Ocean driven by Ekman flow. *Nature 463*, 80–83.

Jimenez-Espejo, F. J., Presti, M., Kuhn, G., Mckay, R., Crosta, X., Escutia, C., Lucchi, R. G., Tolotti, R., Yoshimura, T., Ortega Huertas, M., Caburlotto, A. & De Santis, L. 2020: Late Pleistocene oceanographic and depositional variations along the Wilkes Land margin (East Antarctica) reconstructed with geochemical proxies in deep-sea sediments. *Global Planetary Change 184*, 103045, https://doi.org/10.1016/j.gloplacha.2019.103045.

Jouve, G., Francus, P., Lamoureux, S., Provencher-Nolet, L., Hahn, A., Haberzettl, T., Fortin, D. & Nuttin, L. 2013: Microsedimentological characterization using image analysis and μ-XRF as indicators of sedimentary processes and climate changes during Lateglacial at Laguna Potrok Aike, Santa Cruz, Argentina. *Quaternary Science Reviews 71*, 191–204.

Kasper, T., Frenzel, P., Haberzettl, T., Schwarz, A., Daut, G., Meschner, S., Wang, J., Zhu, L. & Mäusbacher, R. 2013: Interplay between redox conditions and hydrological changes in sediments from Lake Nam Co (Tibetan Plateau) during the past 4000 cal BP inferred from geochemical and micropaleontological analyses. *Palaeogeography, Paleoclimatology, Palaeoecology 392*, 261–271.

Kilian, R. & Lamy, F. 2012: A review of Glacial and Holocene paleoclimate records from southernmost Patagonia (49°S). *Quaternary Science Reviews 53*, 1–23.

Klepeis, K. A. 1994: The Magallanes and Deseado fault zones: major segments of the South American-Scotia transform plate boundary in southernmost South America, Tierra del Fuego. *Journal of Geophysical Research 99*, B11, https://doi.org/10.1029/94JB01749.

Lamy, F., Kilian, R., Arz, H. W., Francois, J. P., Kaiser, J., Prange, M. & Steinke, T. 2010: Holocene changes in the position and intensity of the southern westerly wind belt. *Nature Geoscience 3*, 695–699.

Landscheidt, T. 2000: Solar forcing of El Niño and La Niña. *ESA Special Publication 463*, 135–140.

Laprida, C., Orgeira, M. J., Fernández, M., Tófalo, R., Ramón Mercau, J., Silvestri, G. E., Berman, A. L., García Chapori, N., Plastani, M. S. & Alonso, S. 2021: The role of Southern Hemispheric Westerlies for Holocene hydroclimatic changes in the steppe of Tierra del Fuego (Argentina). *Quaternary International 571*, 11–25.

Leamon, R. J., McIntosh, S. W. & Marsh, D. R. 2021: Termination of solar cycles and correlated tropospheric variability. *Earth and Space Science 8*, e2020EA001223, https://doi.org/10.1029/2020EA001223.

Löwemark, L., Jakobsson, M., Mörth, M. & Backman, J. 2008: Arctic Ocean manganese contents and sediment colour cycles. *Polar Research 27*, 105–113.

Mackay, A., Flower, R., Kuzmina, A., Granina, L., Rose, N., Appleby, P., Boyle, J. & Battarbee, R. 1998: Diatom succession trends in recent sediments from Lake Baikal and their relation to atmospheric pollution and to climate change. *Philosophical Transactions of the Royal Society B Biolological Sciences 353*, 1011–1055.

Makou, M. C., Eglinton, T. I., Oppo, D. W. & Hughen, K. A. 2010: Postglacial changes in El Niño and La Niña behavior. *Geology 38*, 43–46.

Makri, S., Lami, A., Tu, L., Tylmann, W., Vogel, H. & Grosjean, M. 2021: Holocene phototrophic community and anoxia dynam-

ics in meromictic Lake Jaczno (NE Poland) using high-resolution hyperspectral imaging and HPLC data. *Biogeosciences 18*, 1839–1856.
Mansilla, C. A., McCulloh, R. D. & Morello, F. 2016: Palaeoenvironmental change in Southern Patagonia during the Lateglacial and Holocene: implications for forest refugia and climate reconstructions. *Palaeogeography, Palaeoclimatology, Palaeoecology 447*, 1–11.
Mangini, A., Jung, M. & Laukenmann, S. 2001: What do we learn from peaks of uranium and of manganese in deep sea sediments? *Marine Geology 177*, 63–78.
Mariazzi, A. A., Conzonno, V., Ulibarrena, J., Paggi, J. D. & Donadelli, J. L. 1987: Limnological investigation in Tierra del Fuego, Argentina. *Biología Acuática 10*, 44–45.
Markgraf, V. & Huber, U. M. 2010: Late and postglacial vegetation and fire history in Southern Patagonia and Tierra del Fuego. *Palaeogeography, Palaeoclimatology, Palaeoecology 297*, 351–366.
Masiokas, M. & Villalba, R. 2004: Climatic significance of intra-annual bands in the wood of Nothofagus pumilio in southern Patagonia. *Trees: Structure and Function 18*, 696–704.
McCulloch, R., Bentley, M., Purves, R., Hulton, N., Sugden, D. & Clapperton, C. 2000: Climatic inferences from glacial and palaeoecological evidence at the last glacial termination, southern South America. *Journal of Quaternary Sciences 15*, 409–417.
McCulloch, R. D., Blaikie, J., Jacob, B., Mansilla, C. A., Morello, F., De Pol-Holz, R., San Román, R., Tisdall, E. & Torres, J. 2020: Late Glacial and Holocene climate variability, southernmost Patagonia. *Quaternary Science Reviews 229*, 106131, https://doi.org/10.1016/j.quascirev.2019.106131.
Mercer, J. 1976: Glacial history of southernmost South America. *Quaternary Research 6*, 125–166.
Mesa-Fernández, J. M., Jiménez-Moreno, G., Rodrigo-Gamiz, M., García-Alix, A., Jiménez-Espejo, F. J., Martínez-Ruiz, F., Anderson, R. S., Camuera, J. & Ramos-Román, J. 2018: Vegetation and geochemical responses to Holocene rapid climate change in Sierra Nevada (SE Iberia): the Laguna Hondera record. *Climate of the Past 14*, 1687–1706.
Meyers, P. A. 2003: Applications of organic geochemistry to paleolimnological reconstructions: a summary of examples from the Laurentian Great Lakes. *Organic Geochemistry 34*, 261–289.
Meyers, P. A. & Teranes, J. L. 2001: Sediment organic matter. Tracking environmental change using lake sediments. *In* Last, W. & Smol, J. P. (eds.): *Tracking Environmental Change Using Lake Sediments*, 239–269. Kluwer Academic, Dordrecht.
Moreno, P. I., Vilanova, I., Villa-Martínez, R., Garreaud, R. D., Rojas, M. & De Pol-Holz, R. 2014: Southern Annular Mode-like changes in southwestern Patagonia at centennial timescales over the last three millennia. *Nature Communications 5*, 4375, https://doi.org/10.1038/ncomms5375.
Moy, C. M., Dunbar, R. B., Moreno, P. I., Francois, J. P., Villa-Martínez, R., Mucciarone, D. M., Guilderson, T. P. & Garreaud, R. D. 2008: Isotopic evidence for hydrologic change related to the westerlies in SW Patagonia, Chile, during the last millennium. *Quaternary Science Reviews 27*, 1335–1349.
Moy, C. M., Dunbar, R. B., Guilderson, T. P., Waldmann, N., Mucciarone, D. A., Recasens, C., Ariztegui, D., Austin, J. A. & Anselmetti, F. S. 2011: A geochemical and sedimentary record of high southern latitude Holocene climate evolution from Lago Fagnano, Tierra del Fuego. *Earth and Planetary Science Letters 302*, 1–13.
Muñoz, A., Ojeda, J. & Sanchez-Valverde, B. 2002: Sunspot-like and ENSO/NAO-like periodicities in lacustrine laminated sediments of the Pliocene Villarroya Basin (La Rioja, Spain). *Journal of Paleolimnology 27*, 453–463.
Musotto, L. L., Borromei, A. M., Bianchinotti, M. V., Coronato, A., Menounos, B., Osborne, G. & Marr, R. 2017: Postglacial environments in the southern coast of Lago Fagnano, central Tierra del Fuego, Argentina, based on pollen and fungal microfossils analyses. *Review of Palaeobotany and Palynology 238*, 43–54.
Mucciarone, D. A. 2021: *Freeze Drying vs Oven Drying Sediments at 40°C*. Stanford Stable Isotope Lab Facility Internal Laboratory Report, Open Science Framework, https://doi.org/10.17605/OSF.IO/4X765.
Naeher, S., Gilli, A., North, R., Hamann, Y. & Schubert, C. J. 2013: Tracing bottom water oxygenation with sedimentary Mn/Fe ratios in Lake Zurich, Switzerland. *Chemical Geology 352*, 125–133.
Naranjo, J. & Stern, C. 1998: Holocene explosive activity of Hudson Volcano, southern Andes. *Bulletin of Volcanology 59*, 291–306.
Navatini, W. P., Whitlock, C., Iglesias, V. & de Porras, M. E. 2019: Postglacial vegetation, fire, and climate history along the eastern. Andes, Argentina and Chile (lat. 41-55°S). *Quaternary Science Reviews 207*, 145–160.
Neugebauer, I., Thomas, C., Ordoñez, L., Waldmann, N., Recasens, C., Vizcaino, A., Jimenez-Espejo, F. J. & Ariztegui, D. 2022: Preservation of Fe/Mn-redox fronts in sediments of an oligotrophic, oxygenated deep-water lake (Lago Fagnano, Tierra del Fuego). *Sedimentology 69*, 1841–1860.
Onorato, M. R., Perucca, L. P., Coronato, A., Prezzi, C., Blanc, P. A., López, R. & Magneres, I. 2021: Morphotectonic characterization along the eastern portion of the main trace of Magallanes-Fagnano Fault System in Tierra del Fuego, Argentina. *Journal of South American Earth Sciences 112*, 103550, https://doi.org/10.1016/j.jsames.2021.103550.
Pakhomova, S. V., Hall, P. O., Kononets, M. Y., Rozanov, A. G., Tengberg, A. & Vershinin, A. V. 2007: Fluxes of iron and manganese across the sediment–water interface under various redox conditions. *Marine Chemistry 107*, 319–331.
Pedrera, A., Galindo-Zaldívar, J., Ruiz-Constán, A., Bohoyo, F., Torres-Carbonell, P., Ruano, P., Maestro, A. & González-Castillo, L. 2014: The last major earthquakes along the Magallanes–Fagnano fault system recorded by disturbed trees (Tierra del Fuego, South America). *Terra Nova 26*, 448–453.
Pérez-Rodríguez, M. P., Gilfedder, B.-S., Hermanss, Y.-M. & Biester, H. 2016: Solar output controls periodicity in lake productivity and wetness at southernmost South America. *Scientific Reports 6*, 37521, https://doi.org/10.1038/srep37521.
Piccolroaz, S. & Toffolon, M. 2013: Deep water renewal in Lake Baikal: a model for long-term analyses. *Journal of Geophysical Research: Oceans 118*, 6717–6733.
Quade, J. & Kaplan, M. R. 2017: Lake-level stratigraphy and geochronology revisited at Lago (Lake) Cardiel, Argentina, and changes in the Southern Hemispheric Westerlies over the last 25 ka. *Quaternary Science Reviews 177*, 173–188.
Rabassa, J. & Clapperton, C. M. 1990: Quaternary glaciations of the southern Andes. *Quaternary Science Reviews 9*, 153–174.
Raspopov, O., Dergachev, V. & Kolström, T. 2004: Hale cyclicity of solar activity and its relation to climate variability. *Solar Physics 224*, 455–463.
Rees, A. B. H., Cwynar, L. C. & Fletcher, M. S. 2015: Southern westerly winds submit to the ENSO regime: A multiproxy paleohydrology record from Lake Dobson, Tasmania. *Quaternary Science Reviews 126*, 254–263.
Ripepe, M., Roberts, L. T. & Fischer, A. G. 1991: ENSO and sunspot cycles in varved Eocene oil shales from image analysis. *Journal of Sedimentary Petrology 61*, 1155–1163.
Ritcher, A., Hormaechea, J., Dietrich, R., Perdomo, R., Fritsche, M., Del Cogliano, D., Liebsch, G. & Mendoza, L. 2010: Lake-level variations of Lago Fagnano, Tierra del Fuego: observations, modelling and interpretation. *Journal of Limnology 69* (1), 29–41.
Rogers, J. C. & van Loon, H. 1982: Spatial variability of sea level pressure and 500 mb height anomalies over the Southern Hemisphere. *Monthly Weather Review 110*, 1375–1392.
Rowe, M. D., Anderson, E. J., Beletsky, D., Stow, C. A., Moegling, S. D., Chaffin, J. D., May, J. C., Collingsworth, P. D., Jabbari, A. & Ackerman, J. D. 2019: Coastal upwelling influences hypoxia spatial patterns and nearshore dynamics in Lake Erie. *Journal Geophysical Research: Oceans 124*, 6154–6175.
Rush, R. A. 2010: *High resolution geochemical XRF data from Elk Lake, Minnesota: A Holocene paleoclimate record from varved lake sediment*. M.S. thesis, University of Minnesota Duluth, 138 pp.
Rutten, A., de Lange, G. J., Hayes, A., Rohling, E. J., de Jong, A. F. M. & van der Borg, K. 1999: Deposition of sapropel S1 sediments in oxic pelagic and anoxic brine environments in the eastern Mediterranean: differences in diagenesis and preservation. *Marine Geology 153*, 319–335.

Sanci, R., Orgeira, M. J., Coronato, A., Tófalo, R., Panarello, H. O., Quiroga, D., López, R., Palermo, P. & Gogorza, C. S. 2021: Late Pleistocene glaciolacustrine MIS 3 record at Fagnano Lake, Central Tierra del Fuego, southern Argentina. *Quaternary Research 102*, 53–67.

Saunders, K. M., Roberts, S. J., Perren, B., Butz, C., Sime, L., Davies, S., van Nieuwenhuyze, W., Grosjean, M. & Hodgson, D. A. 2018: Holocene dynamics of the Southern Hemisphere westerly winds and possible links to CO_2 outgassing. *Nature Geoscience 11*, 650–655.

Schaller, T., Moor, H. C. & Wehrli, B. 1997: Sedimentary profiles of Fe, Mn, V, Cr, As and Mo as indicators of benthic redox conditions in Baldeggersee. *Aquatic Science 59*, 345–361.

Schaller, T. & Wehrli, B. 1997: Geochemical-focusing of manganese in lake sediments - an indicator of deep-water oxygen conditions. *Aquatic Geochemistry 2*, 359–378.

Schneider, C. & Gies, D. 2004: Effects of El Niño southern oscillation on southernmost South America precipitation at 53 S revealed from NCEP NCAR reanalyses and weather station data. *International Journal of Climatology 24*, 1057–1076.

Smalley, R., Kendrick, E., Bevis, M., Dalziel, I., Taylor, F., Lauría, E., Barriga, R., Casassa, G., Olivero, E. & Piana, E. 2003: Geodetic determination of relative plate motion and crustal deformation across the Scotia-South America plate boundary in eastern Tierra del Fuego. *Geochemistry, Geophysics, Geosystems 4*, 1070, https://doi.org/10.1029/2002GC000446.

Stern, C. R. 2008: Holocene tephrochronology record of large explosive eruptions in the southernmost Patagonian Andes. *Bulletin of Volcanology 70*, 435–454.

Stern, C., Moreno, I. P., Henríquez, W. I., Villa-Martínez, R., Sagredo, E., Aravena, J. C. & de Pol-Holz, R. 2016: Holocene tephrochronology around Cochrane (~47°S), southern Chile. *Andean Geology 43*, 1–19.

Stow, D. A. V. & Zeinab, S. 2020: Distinguishing between deep-water sediment facies: turbidites, contourites and hemipelagites. *Geosciences 10*, 68, https://doi.org/10.3390/geosciences10020068.

Stuiver, M., Reimer, P. J. & Reimer, R. W. 2021: *CALIB 8.2* (WWW program) Available at: http://calib.org (accessed 2021-5-25).

Turney, C. S. M., Jones, R. T., Fogwill, C., Hatton, J., Williams, A. N., Hogg, A., Thomas, Z. A., Palmer, J., Mooney, S. & Reimer, R. W. 2016: A 250-year periodicity in Southern Hemisphere westerly winds over the last 2600 years. *Climate of the Past 12*, 189–200.

Toggweiler, J., Russell, J. & Carson, S. 2006: Midlatitude westerlies, atmospheric CO_2, and climate change during the ice ages. *Paleoceanography 21*, PA2005, https://doi.org/10.1029/2005PA001154.

Waldmann, D. N., Ariztegui, D., Anselmetti, F. S., Austin, J. A., Jr., Dunbar, R. B., Moy, C. M. & Recasens, C. 2008: Seismic stratigraphy of Lago Fagnano sediments (Tierra del Fuego, Argentina)-A potencial archive of paleoclimatic change and tectonic activity since the Late Glacial. *Geologica Acta 6*, 101–110.

Waldmann, N., Ariztegui, D., Anselmetti, F. S., Austin, J. A., Moy, C. M., Stern, C., Recasens, C. & Dunbar, R. B. 2010: Holocene climatic fluctuations and positioning of the Southern Hemisphere westerlies in Tierra del Fuego (54°S), Patagonia. *Journal of Quaternary Science 25*, 1063–1075.

Waldmann, N., Anselmetti, F. S., Ariztegui, D., Austin, J. A., Pirouz, M., Moy, C. M. & Dunbar, R. 2011: Holocene mass-wasting events in Lago Fagnano, Tierra del Fuego (54°S): implications for paleoseismicity of the Magallanes-Fagnano transform fault. *Basin Research 23*, 171–190.

Waldmann, N., Borromei, A. M., Recasens, C., Olivera, D., Martínez, M. A., Maidana, N. I., Ariztegui, D., Austin, J. A., Anselmetti, F. S. & Moy, C. M. 2014: Integrated reconstruction of Holocene millennial-scale environmental changes in Tierra del Fuego, southernmost South America. *Palaeogeography, Palaeoclimatology, Palaeoecology 339*, 294–309.

Weltje, G., Bloemsma, M., Tjallingii, R., Heslop, D., Röhl, U. & Croudace, I. 2015: Prediction of geochemical composition from XRF core scanner data: a new multivariate approach including automatic selection of calibration samples and quantification of uncertainties. *In* Croudace, I. & Rothwell, R. (eds.): *Micro-XRF Studies of Sediment Cores*, 507–534. Springer, Dordrecht.

Weiss, R. F., Carmack, E. C. & Koropalov, V. M. 1991: Deep-water renewal and biological production in Lake Baikal. *Nature 349*, 665–669.

Xia, Z., Yu, Z. & Loisel, J. 2018: Centennial-scale dynamics of the Southern Hemisphere Westerly Winds across the Drake Passage over the past two millennia. *Geology 46*, 855–858.

Zolitschka, B., Fey, M., Janssen, S., Maidana, N. I., Mayr, C., Wulf, S., Haberzettl, T., Corbella, H., Lücke, A., Ohlendorf, C. & Schäbitz, F. 2019: Southern Hemispheric Westerlies control sedimentary processes of Laguna Azul (south-eastern Patagonia, Argentina). *The Holocene 29*, 403–420.